An ATM/Chk2-Mediated DNA Damage-Responsive Signaling Pathway Suppresses Epstein-Barr Virus Transformation of Primary Human B Cells

Pavel A. Nikitin,[1,4] Christopher M. Yan,[1,4] Eleonora Forte,[1,5] Alessio Bocedi,[1] Jason P. Tourigny,[1] Robert E. White,[2] Martin J. Allday,[2] Amee Patel,[3] Sandeep S. Dave,[3] William Kim,[3] Katherine Hu,[1] Jing Guo,[1] David Tainter,[1] Elena Rusyn,[1] and Micah A. Luftig[1,*]

[1]Department of Molecular Genetics and Microbiology, Center for Virology, Duke University School of Medicine, Durham, NC 27712, USA
[2]Department of Virology, Faculty of Medicine, Imperial College London, Norfolk Place, London W2 1PG, UK
[3]Duke Institute for Genome Sciences and Policy, Duke University, Durham, NC 27712, USA
[4]These authors contributed equally to this work
[5]Present address: Division of Infectious Diseases, Department of Internal Medicine, University of Utah, Salt Lake City, UT 84132, USA
*Correspondence: micah.luftig@duke.edu
DOI 10.1016/j.chom.2010.11.004
Open access under CC BY license.

SUMMARY

Epstein-Barr virus (EBV), an oncogenic herpesvirus that causes human malignancies, infects and immortalizes primary human B cells in vitro into indefinitely proliferating lymphoblastoid cell lines, which represent a model for EBV-induced tumorigenesis. The immortalization efficiency is very low, suggesting that an innate tumor suppressor mechanism is operative. We identify the DNA damage response (DDR) as a major component of the underlying tumor suppressor mechanism. EBV-induced DDR activation was not due to lytic viral replication, nor did the DDR marks colocalize with latent episomes. Rather, a transient period of EBV-induced hyperproliferation correlated with DDR activation. Inhibition of the DDR kinases ATM and Chk2 markedly increased transformation efficiency of primary B cells. Further, the viral latent oncoprotein EBNA3C was required to attenuate the EBV-induced DDR. We propose that heightened oncogenic activity in early cell divisions activates a growth-suppressive DDR that is attenuated by viral latency products to induce cell immortalization.

INTRODUCTION

Epstein-Barr virus (EBV) is an oncogenic herpesvirus causally implicated in several malignancies including African endemic Burkitt's lymphoma (BL), posttransplant lymphoproliferative disease, nasopharyngeal carcinoma, and HIV-associated lymphomas (Kieff and Rickinson, 2006). EBV infection in vitro drives primary human B cells into indefinitely proliferating lymphoblastoid cell lines (LCLs), providing a model for tumorigenesis. This process of growth transformation depends on a subset of viral latent oncoproteins and noncoding RNAs collectively termed "latency III." The proteins expressed include the Epstein-Barr nuclear antigens, EBNA1, -2, -3A, -3B, -3C, and -LP as well as

three latent membrane proteins, LMP1, -2A, and -2B. EBNA-LP and EBNA2 are the first viral proteins expressed following primary B cell infection (Alfieri et al., 1991) and upregulate cellular genes inducing a transition of resting B cells into the cell cycle (Sinclair et al., 1994; Wang et al., 1991). EBNA2 also induces expression of the remaining EBNA proteins (Zimber-Strobl et al., 1993) and subsequently the viral latent membrane proteins, LMP1 and LMP2A/2B (Wang et al., 1990).

While the initial burst of viral and cellular gene expression leads to the proliferation of infected cells in vitro, only a small percentage of infected cells become indefinitely proliferating lymphoblasts (Henderson et al., 1977; Sugden and Mark, 1977). The study of EBV-induced innate tumor suppressor pathways has been limited. EBV infection of primary B cells induces the p53 protein concomitant with EBNA-LP expression early after infection (Szekely et al., 1995). However, it remains unclear whether this innate response to EBV-induced proliferation has any long-term functional consequence or what pathways activate p53.

Innate tumor suppressor responses have been better characterized in other systems. The DNA damage response (DDR) has recently been appreciated as an important tumor suppressor pathway in vitro and in vivo (Bartkova et al., 2005; Gorgoulis et al., 2005). The DDR is triggered by aberrant replication structures generated by activated oncogenes attempting to constitutively fire new origins and inappropriately enter S phase (Halazonetis et al., 2008). The DDR limits aberrant proliferation by mediating oncogene-induced senescence and apoptosis (Bartkova et al., 2006; Di Micco et al., 2006). Signaling downstream of oncogenic stress involves activation of the single-stranded DNA-dependent ATR pathway and the double-stranded break-induced ATM pathway. These DDR kinases relay downstream signals to critical repair factors and other checkpoint kinases including Chk1 and Chk2 with extensive crosstalk ultimately resulting in suppression of oncogene-induced proliferation (Halazonetis et al., 2008; Stiff et al., 2006). Genetic experiments have identified critical roles for ATM and Chk2 in mediating oncogene-induced senescence and tumor suppression (Bartkova et al., 2006; Pusapati et al., 2006; Stracker et al., 2008). Given these observations and the low
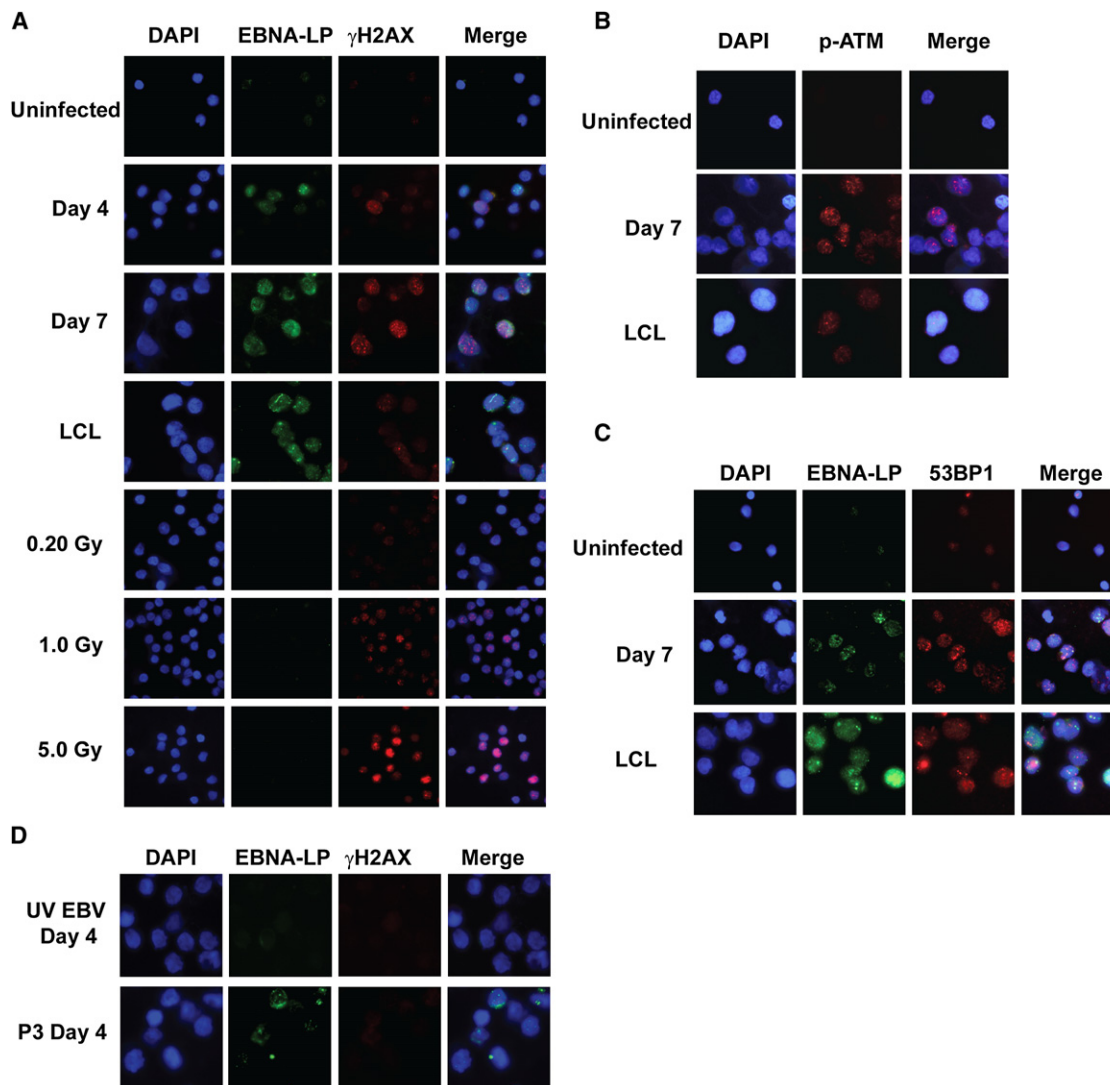
Figure 1. EBV Induced a DNA Damage Response in Primary B Cells

(A) Indirect IF images of EBNA-LP (green) and γ-H2AX (red) in uninfected B cells, B cells 4 and 7 days after infection with EBV B95-8 (moi $\sim$5), the recently derived LCL EF3D, and uninfected γ-irradiated B cells (0.2, 1, and 5 Gy, 1 hr). DNA is stained with DAPI. These images are representative of infections in five different normal donors.

(B) Ser1981 phosphorylated ATM (pATM, red) in uninfected B cells and B cells 7 days after EBV B95-8 infection. EBNA-LP or other EBV latent antigen staining was not possible in these samples due to antibody source; however, we know that the majority of these infected cells are EBNA-LP positive.

(C) EBNA-LP (green) and 53BP1 (red) in uninfected B cells and B cells 7 days after infection.

(D) EBNA-LP (green) and γ-H2AX (red) in B cells 4 days after infection with UV-inactivated EBV B95-8 (UV EBV) or the nontransforming EBV strain P3HR1 (P3).

efficiency of EBV transformation, the intriguing question remains as to whether the host DDR senses EBV-induced oncogenic stress and, importantly, if this is responsible for the block to long-term outgrowth of the majority of infected cells.

RESULTS

Epstein-Barr Virus Infection of Primary B Cells Activates a Cellular DNA Damage Response

We first sought to determine whether EBV infection of primary B cells might drive an oncogenic stress leading to the activation of the DDR. Purified CD19+ B cells were infected with the proto-typical transforming EBV strain B95-8 at a multiplicity of infection (moi) of $\sim$5. Nearly all cells were EBV genome positive as determined by fluorescence in situ hybridization (FISH) (see Figure S1A available online). Infected cells were initially assayed for the expression of the earliest viral latency gene product, EBNA-LP (LP), and the DNA damage marker, γ-H2AX, at different times postinfection. γ-H2AX activation was not evident prior to 4 days postinfection, was robust from 4 to 7 days post-infection, and declined after 7 days to the low levels observed in LCLs (Figure 1A and data not shown). Approximately 60% of the infected cells were γ-H2AX positive at 7 days postinfection. Corroborating our findings of γ-H2AX activation, EBV infection

induced additional hallmarks of the DDR including autophosphorylation of the H2AX kinase ATM (pATM Ser1981), and punctate localization of the damage adaptor 53BP1 (Figures 1B and 1C).

EBV gene expression was important for virus-induced DDR activation. Cells infected with UV-inactivated B95-8 virus did not show γ-H2AX staining at any point within the first week after infection (Figure 1D and data not shown). Importantly, UV-inactivated EBV B95-8 genomes reached the nucleus, and these infections induced interferon-responsive genes (Figures S1A and S1B). EBNA2 and latency III gene expression was specifically necessary to induce the DDR, as B lymphocytes infected with the EBNA2-deleted, transformation-incompetent P3HR1 strain of EBV did not contain γ-H2AX foci (Figure 1D), despite similar levels of infection compared to B95-8 (Figures S1A and S1C). These data collectively demonstrate that EBV latent gene expression, rather than simply virion binding or nucleic acid deposition into the nucleus, was required to induce γ-H2AX activation.

The EBV-Induced DNA Damage Response in Primary B Cell Infection Is Not Associated with Viral Episomes or Lytic Replication

We reasoned that either viral or cellular DNA may activate the DDR. Since evidence in the literature suggested that either viral lytic DNA replication (Kudoh et al., 2005) or latent viral episome replication (Dheekollu et al., 2007) may be capable of inducing a DDR, we first assayed viral DNA as a possible source of the damage. Incoming linear viral DNA was not the source of the damage, since UV-irradiated and EBNA2-deleted P3HR1 virus infections did not induce the DDR (Figure 1). We next used a FISH-based assay to assess the possible role of lytic DNA replication. The B95-8 Z-HT cell line was used as a positive control where lytic EBV DNA was recognized as a brightly staining FISH signal rather than the punctate foci of episomal genomes (Figure S1D). Less than 1% of EBV-infected cells contained evidence of lytic viral DNA 5 days postinfection, while ∼1%–5% of infected cells were spontaneously undergoing lytic replication by 14 days, similar to that found in LCLs (Figure S1E and Kieff and Rickinson, 2006). Since far greater than 1% of EBV-infected cells were γ-H2AX positive early after infection, we conclude that viral lytic DNA replication is not responsible for DDR activation.

Next we assessed the possibility that latent viral episomes activate the DDR. The mean episome number per cell as assessed by FISH did not increase during the period when γ-H2AX activity was high early after infection (Figure S1F). Furthermore, we failed to observe significant colocalization of EBV episomes with γ-H2AX foci in these cells (Figure S1G). In fact, the number of γ-H2AX foci per cell was consistently much greater than the number of EBV genomes (Figure S1G). Therefore, our data collectively suggest that the observed EBV-induced DDR is not activated by viral DNA.

The EBV-Induced DNA Damage Response Is Associated with a Transient Period of Hyperproliferation

We next focused our studies on changes in cellular DNA that may induce a DDR. The period of time postinfection when the DDR was active correlates with the initiation of B cell proliferation

(Kieff and Rickinson, 2006). Analysis of CD19+ B cells using the proliferation-tracking dye CFSE at different days after infection indicated that (1) proliferating cells appeared at day 3 (Figure 2A), (2) between days 3 and 4 there were always cells that had divided more than once or even twice in 24 hr, and (3) at later days postinfection cells appeared to proliferate at a slower rate as judged by the less-pronounced shift of the CFSE profile to the left.

A more rigorous kinetic analysis of EBV-induced B cell expansion highlighted the biphasic nature of the proliferation rate (Figure 2B). Infected CD19+ B cell CFSE profiles from five normal donors were analyzed at time points prior to and during the first seven cell divisions. The mean division number (MDN) at each time point was determined by fitting the precursor-normalized number of cells in each division to a Gaussian distribution (Figure S2A and Hawkins et al., 2007). The slope of the function relating MDN to time postinfection inversely correlates with the proliferation rate. Consistent with the data in Figure 2A, we observed that EBV induced an early phase of hyperproliferation that was attenuated over time (Figure 2B). The proliferation rate of initially proliferating cells was approximately once per 8–12 hr, while later cycles were ∼24–30 hr, similar to the ∼24–28 hr rate of LCLs. These findings were corroborated by cell-sorting experiments where cells from earlier divisions proliferated more quickly than those in later divisions (Figure S2B). Thus, EBV-mediated B cell expansion proceeds through an initial period of hyperproliferation followed by slower cell divisions typical of emergent LCLs.

We next asked whether the DDR was activated specifically during the hyperproliferative divisions independent of time postinfection. EBV-infected B cells sorted based on population doubling (PD) were subjected to immunofluorescence (IF) for EBNA-LP and γ-H2AX (Figure 2C). Sorted cells were >85% EBNA-LP positive in cells not yet dividing (PD0) and >95% EBNA-LP positive in all later PDs. We observed a robust increase in LP$^+$/γ-H2AX$^+$ cells during the early PDs (1–2 and 3–4) relative to uninfected cells or infected cells not yet proliferating (PD0) (Figures 2C and 2D). Importantly, this response was attenuated through later PDs and in LCLs. Moreover, γ-H2AX intensity per cell was significantly higher in PD3-4 than PD0 (p < 0.0001) and LCL (p < 0.0001). We also observed a transient activation and attenuation of the ATM-specific phosphorylation of Chk2 on Thr68 (Figure 2E) as well as accumulation of 53BP1 into DDR foci (Figure 2F). These data strongly support the notion that the EBV-induced DDR is caused by an early period of hyperproliferation and is attenuated during LCL outgrowth.

Proliferation and DNA Damage-Responsive Genes Are Highly Induced Early after EBV Infection, then Attenuated during LCL Outgrowth

Our cell-based findings were corroborated by mRNA microarray studies of (1) uninfected B cells, (2) EBV-infected early proliferating cells (Prolif), and (3) monoclonal LCLs from four normal donors (Figure 3). We first asked in an unbiased manner which genes were significantly changed upon proliferation and then, subsequently, during LCL outgrowth (two-way ANOVA, p < 0.01). As expected, the most enriched gene ontology (GO) category for genes induced from resting B cells to EBV-infected,
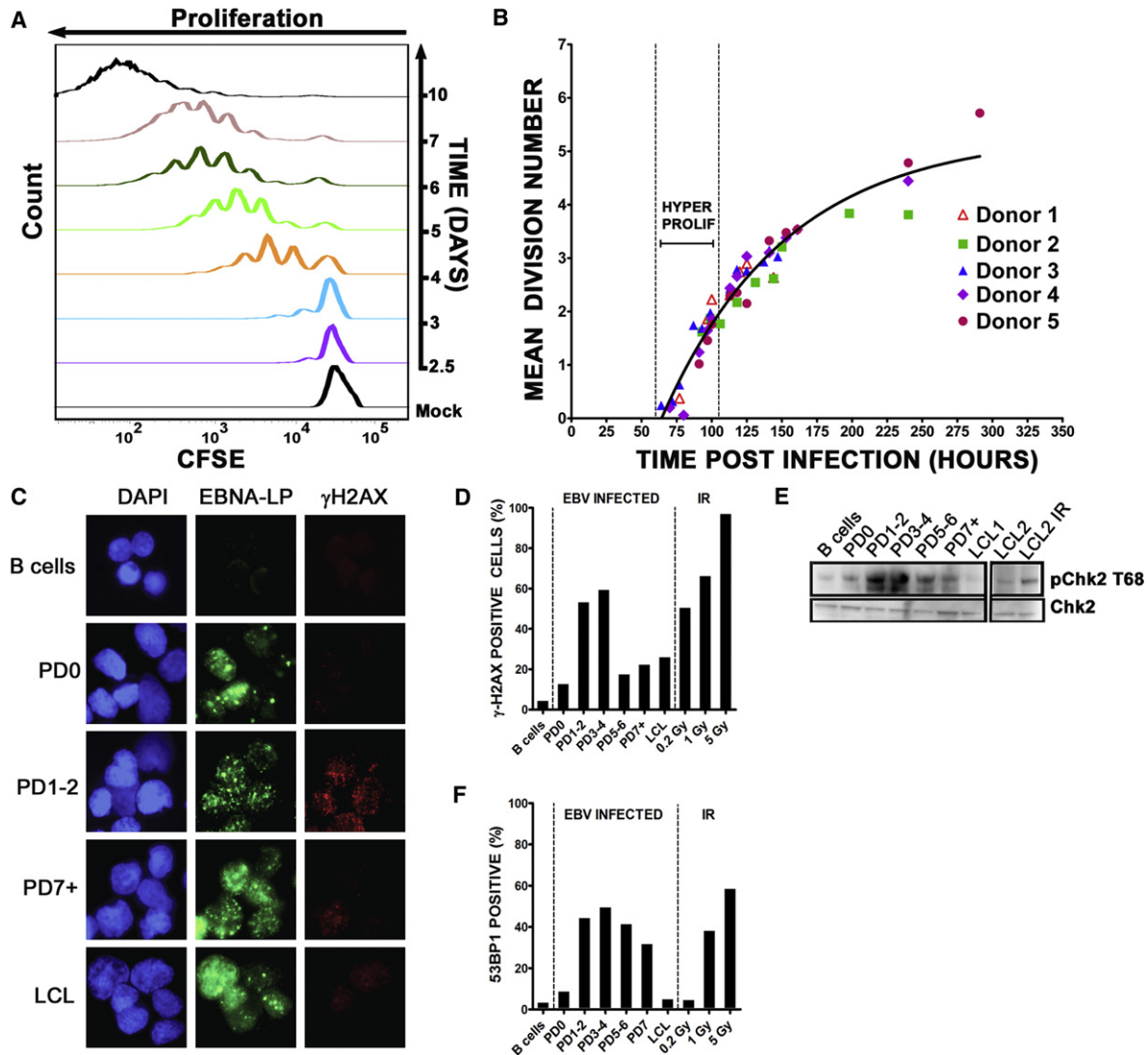
Figure 2. EBV Induced a Period of Hyperproliferative Early after Infection that Was Associated with Activation of the DNA Damage Response
(A) Histograms show CD19+ B cell division as measured by CFSE staining at different days after EBV infection. Mock, mock infected cells.
(B) The MDN based on precursor cohort analysis for EBV-infected B cells is plotted at different times post infection. Vertical dashed lines estimate the hyper-proliferation period. Data are presented from five normal donors.
(C) IF of γ-H2AX (red) and EBNA-LP (green) in uninfected cells, infected cells that have yet to divide (PD0), infected cells after one or two divisions (PD1-2), or seven or more divisions (PD7+) and LCLs. DNA is stained with DAPI.
(D) The percentage of EBNA-LP-positive cells with γ-H2AX signal >5× over background is graphed from uninfected B cells, sorted PDs, and LCLs. Uninfected B cells following 0.2, 1, and 5 Gy (1 hr) γ-irradiation are also shown as a positive control. These data are representative of similar experiments from three independent normal donors.
(E) Immunoblot of p-Chk2 Thr68 and Chk2 in sorted cells as in (D) including an LCL following 5 Gy γ-irradiation (1 hr).
(F) The percentage of EBNA-LP-positive cells containing four or more 53BP1 foci per cell in sorted populations as in (D) are shown along with uninfected irradiated B cell controls. PD3-4 contained significantly more 53BP1 foci per cell than uninfected B cells (p < 0.0001), PD0 (p < 0.0001), PD7 (p < 0.01), and LCL (p < 0.0001).

proliferating B cells was "Cell Proliferation" (Figure 3A; GO, 0008283; Bayes factor, 51, p < 0.0001 [Chang and Nevins, 2006]). Genes associated with the "Response to DNA Damage Stimulus" were also highly induced (Figure 3B; GO, 0006974; Bayes factor, 17, p < 0.0001). Notably, we observed that the majority of genes involved in cell proliferation and the DDR were consistently repressed as cells transitioned from early proliferating to established LCLs (Figure 3A, "Cell Proliferation,"

Bayes factor, 63, p < 0.0001 and Figure 3B, "Response to DNA Damage Stimulus," Bayes factor, 22, p < 0.0001). Consistently, the expression of genes in an independently derived set of DNA damage responsive and ATM-dependent p53 targets (Elkon et al., 2005) was also increased in early proliferating cells and subsequently attenuated during LCL outgrowth (Figure 3C and Figure S3). Collectively, these global gene expression analyses corroborate our findings of a period of hyperproliferation and
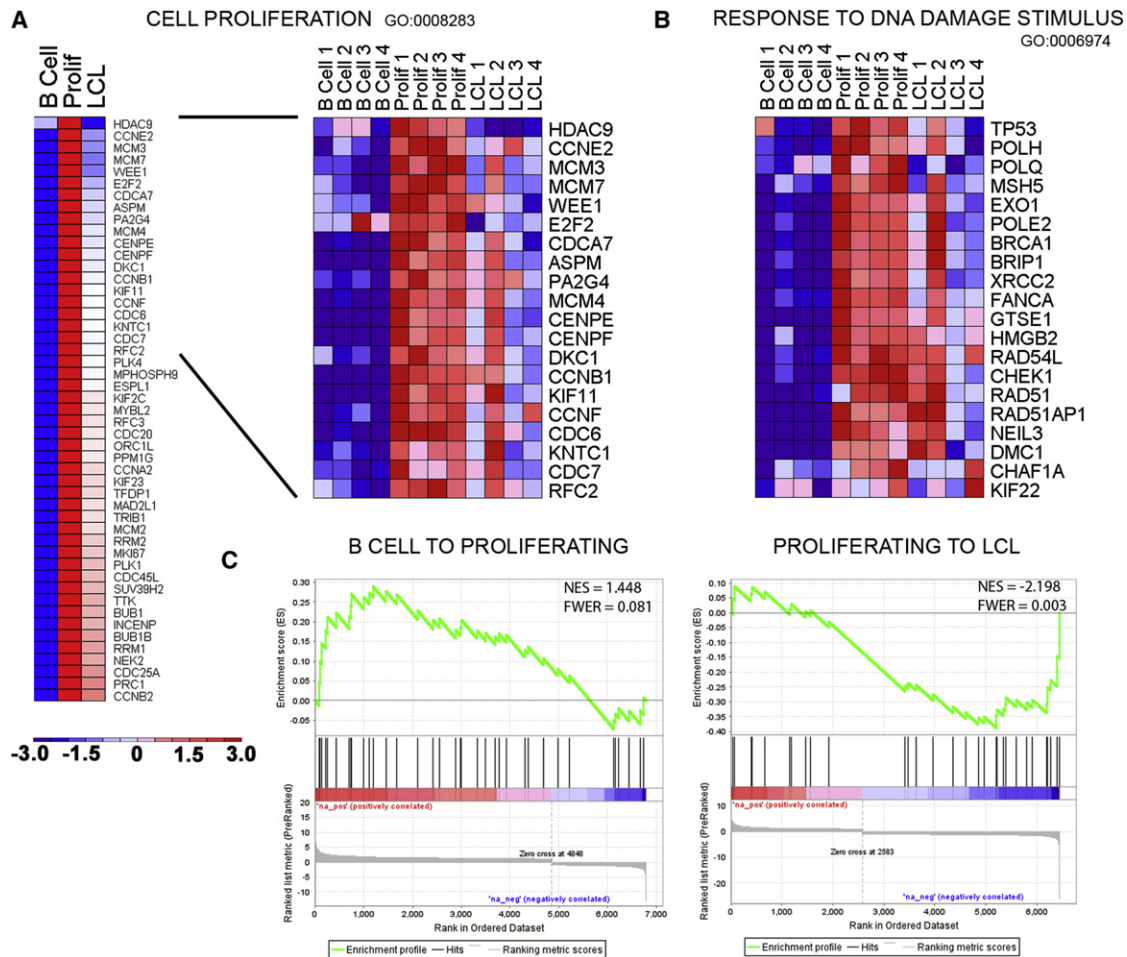
Figure 3. Transcriptional Changes Correlate with an EBV-Induced Early Period of Hyperproliferation and DNA Damage Response Followed by Attenuation upon LCL Outgrowth

(A) Heat map of average expression data across four normal donors for the GO category "Cell Proliferation" in uninfected resting B cells (B cell), EBV-infected early proliferating B cells (Prolif), and monoclonal LCLs (LCL). The genes presented were derived from GATHER analysis of all genes with significant expression changes (two-way ANOVA, p < 0.01) where the expression level increased from B cell to Prolif at least 1.5-fold and decreased from Prolif to LCL at least 1.2-fold (left). Heat map of individual samples of top 20 "Cell Proliferation" genes (right).

(B) Heat map of "Response to DNA Damage Stimulus" GO genes across individual samples.

(C) Gene Set Enrichment Analysis (GSEA) of known DNA damage induced ATM and p53-dependent genes in the context of B-Prolif-LCL expression data. The reference list of ATM/p53 target genes was derived from clusters 2 and 3 of Elkon et al. (2005) and compared with a preranked list (by fold) of global average gene expression changes from B cell to Prolif (left) and Prolif to LCL (right). Statistical scores are inset into the top right of analysis images (NES, normalized enrichment score; and FWER, familywise error rate).

---

activation of an ATM-dependent DDR early after infection that is attenuated during LCL outgrowth.

The EBV-Induced Hyperproliferation-Associated DNA Damage Response Is Growth Suppressive

To further analyze the consequences of the activated DDR in early rapidly proliferating cells, we designed a sorting strategy to assess the relative growth potential and DDR activation in cells derived from early or late divisions after infection (Figure 4A). We initially stained cells with the proliferation tracking dye PKH26 and sorted cells after infection for PD1-4 and PD6+ populations (Figure 4B). Subsequent staining with CFSE enabled the analysis of proliferation from these populations. Supporting our hypothesis, the cells in early hyperproliferating divisions

(PD1-4) were, in fact, more prone to growth arrest and cell death than those in later divisions (PD6+) and LCLs (Figure 4C). Consistently, arrested PD1-4 cells displayed more intense γ-H2AX staining than their proliferating counterparts (Figure 4D).

ATM and Chk2 Kinases Suppress EBV-Mediated Transformation and Initial B Cell Proliferation

To determine if the activation of the DDR restricts EBV-mediated long-term outgrowth, we simultaneously infected peripheral blood mononuclear cells (PBMCs) with EBV and treated them with an inhibitor of either ATM (ATMi [Hickson et al., 2004]) or its downstream effector kinase Chk2 (Chk2i [Arienti et al., 2005]); both are critical kinases in the DDR checkpoint responding to DNA double-stranded breaks and oncogenic stress.
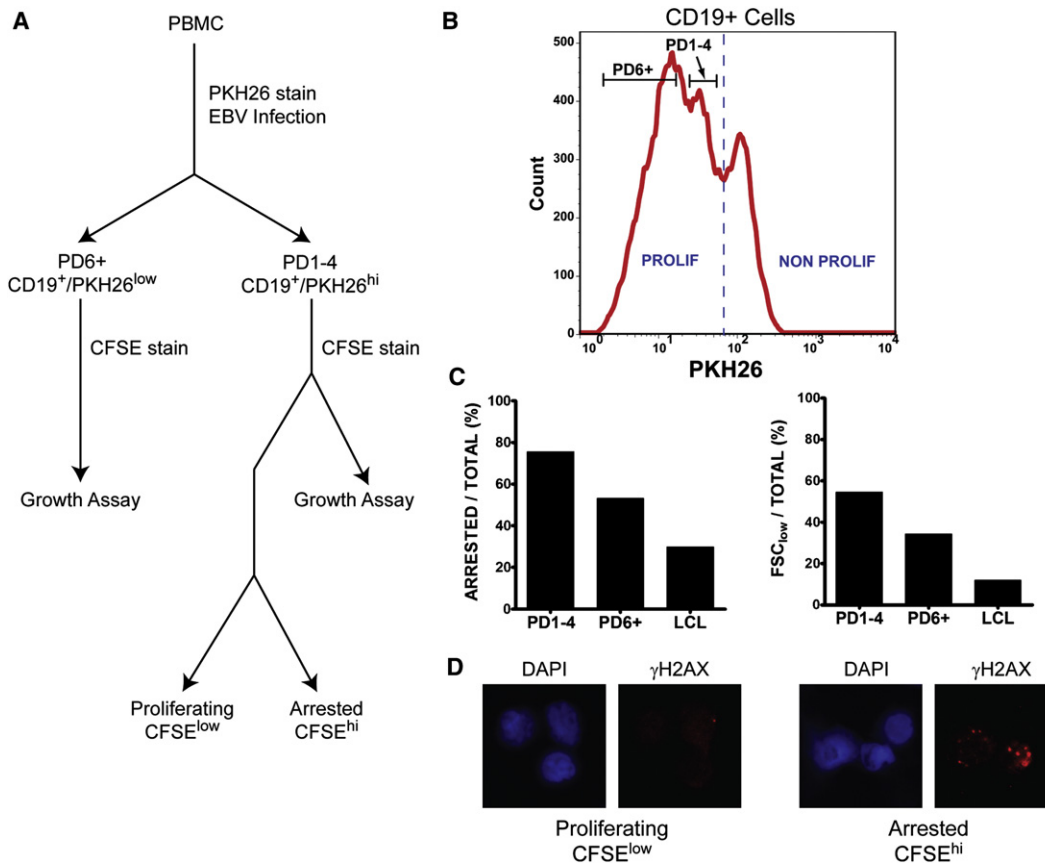
Figure 4. Growth Suppression and DNA Damage Enrichment in Early Cell Divisions

(A) A flowchart shows the separation of arrested and proliferating EBV-infected CD19+ PBMCs used for IF and FACS. PBMCs were first infected with EBV and labeled with the red fluorescent dye PKH26.

(B) Then, 8 days postinfection, proliferating CD19+ B cells were sorted for PD1-4 and PD6+ based on PKH26 intensity, labeled with CFSE, and cultured for 2 days.

(C) Sorted cells were then analyzed in a FACS-based growth assay where cells in the CFSE^{low} population were considered proliferating and cells in the CFSE^{hi} population were considered arrested. Forward scatter (FSC) low reflects dying cells. Results are representative of three normal donors.

(D) PKH26^{low} (PD1-4) cells were subsequently labeled with CFSE as above, sorted after 48 hr in culture into CFSE^{hi} (arrested) and CFSE^{low} (proliferating) populations, and analyzed by IF for γ-H2AX (red).

EBV-mediated B cell transformation efficiency increased in a dose-dependent manner in response to the inhibitors where 2 μM ATMi increased efficiency by ~2-fold and 5 μM ATMi by 6-fold over DMSO control-treated cells (Figure 5A). Similarly, Chk2 inhibition increased EBV transformation efficiency ~3-fold for 2 μM Chk2i and 9-fold for 5 μM Chk2i (Figure 5B). Therefore, an ATM- and Chk2-dependent DDR restricts EBV transformation.

We next assessed whether ATM and Chk2-mediated suppression of EBV transformation was due to limiting initial B cell proliferation. The continuous presence of either ATM or Chk2 inhibitor led to a dose-dependent increase in infected B cell number at 2 weeks postinfection (Figure 5C). Importantly, ATM or Chk2 inhibitor did not induce B cell proliferation in the absence of EBV, suggesting that these compounds act to alleviate a block to proliferation rather than stimulating B cells per se (Figure 5D).

ATM and Chk2 Suppress B Cell Growth 4–8 Days after EBV Infection

Since the DDR peaked during the first week after infection, we assessed when ATM and Chk2 inhibition enhanced proliferation and transformation. To that end, PBMCs infected with EBV were transiently exposed to ATMi and Chk2i from the start of infection or the compounds were added at different days postinfection. EBV-induced B cell proliferation was most sensitive to the inhibitors between 4 and 8 days after infection when cells were present in the hyperproliferative period (Figure 5E). For example, when either inhibitor was added within the first 4 days of infection, we observed as pronounced an effect on proliferation as if the inhibitor was added at day 0. However, if we added inhibitors after day 8, there was no effect on proliferation. Conversely, if the inhibitors were removed prior to 4 days after infection, then increased proliferation was not observed.

Similar results were obtained in long-term transformation assays. Addition of either compound within 4 days of infection increased transformation efficiency, while adding the compounds at 12 days postinfection had little effect (Figures 5F and 5G). The inhibitors also did not increase LCL growth rates at normal or limiting density (Figure S4 and data not shown). Therefore, during a critical period ~4–8 days following infection, EBV induced an ATM- and Chk2-dependent growth suppressive
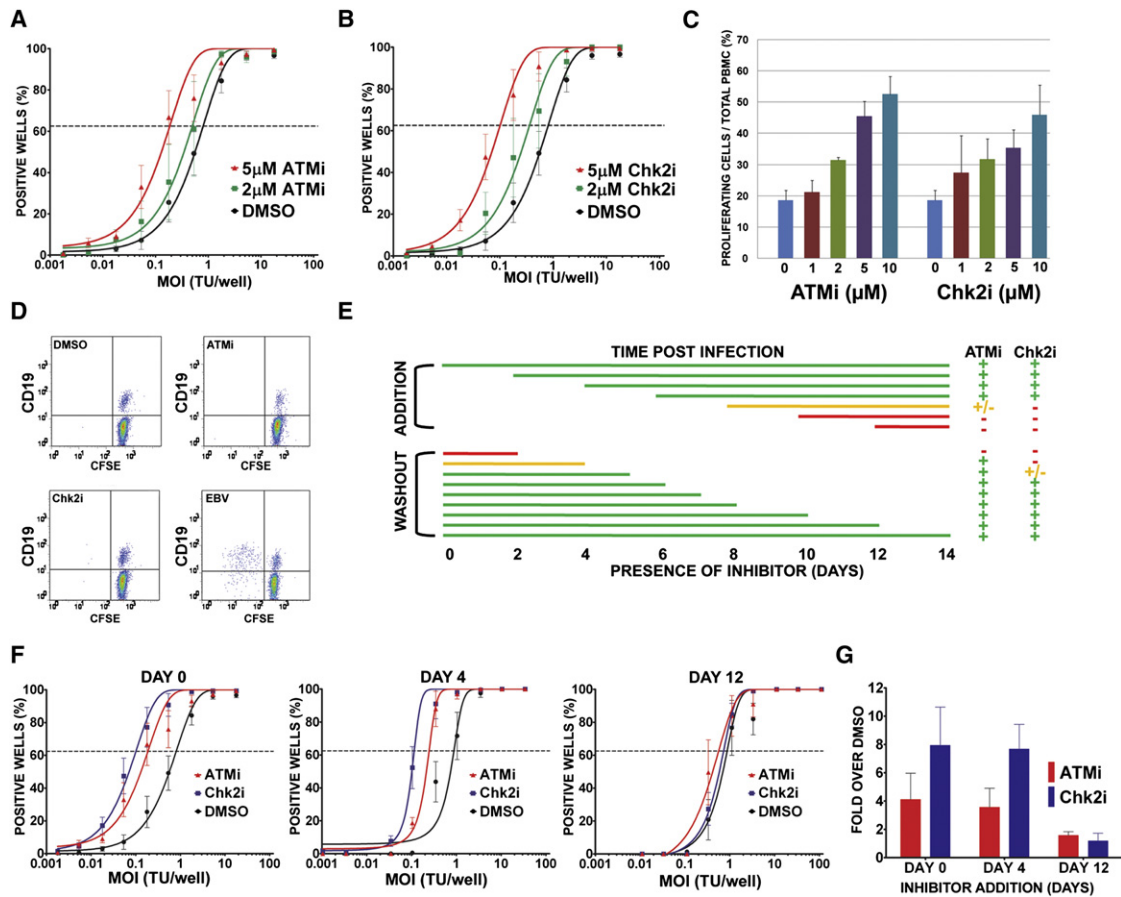
Figure 5. Inhibition of ATM and Chk2 Kinases Increased EBV Transformation Efficiency and Proliferation of B Cells during a Critical Period 4–8 Days Postinfection

(A) Quantification of EBV-induced B cell outgrowth following PBMC infection in the presence of 0.1% DMSO (black), 2 μM ATMi (green), or 5 μM ATMi (red). The percentages of wells positive for LCLs at 5 weeks postinfection are plotted relative to the transforming units (TU) of B95-8 virus per well. Results shown are the average of experiments with at least four independent normal donors. Error bars represent standard error of the mean (SEM). Dotted line represents 62.5% positive wells, which, based on a Poisson's distribution, indicates outgrowth from the virus amount in the x axis of a single LCL per well.

(B) Similar experiments were performed as in (A), except using DMSO (black), 2 μM Chk2i (green), or 5 μM Chk2i (red).

(C) CFSE-stained PBMCs were infected with EBV in the presence of increasing amounts of ATMi or Chk2i (0, 1, 2, 5, and 10 μM). The percentage of CD19$^+$/CFSE-^{low} cells of total PBMCs at 14 days postinfection are plotted. The data shown are the average values from two different donors ± SEM. These data are representative of more than five independent experiments.

(D) Dot plots show CFSE- and CD19-stained PBMCs that were treated with DMSO, 5 μM ATMi, or 5 μM Chk2i or infected with EBV for 6 days.

(E) This table summarizes when ATM and Chk2 suppressed EBV-mediated proliferation at different times following infection. CFSE-stained PBMCs were infected with EBV at day 0. ATMi or Chk2i (5 μM) was added at different times after infection (top bars) or at day 0 and washed out at different times after infection (bottom bars). EBV-mediated B cell proliferation was detected by FACS at day 14 postinfection using CD19-PE and CFSE as in (C). A more than 2-fold increase in treated cells versus DMSO is represented by a green plus, a less than 2-fold increase is represented by a yellow plus, and no increase is represented by a red dash. The lines indicate the period of incubation and are colored with the proliferation phenotype after ATMi and Chk2i treatment. Average values from two independent donors are shown.

(F) EBV-induced outgrowth following PBMC infection was measured as in (A) in the presence of 5 μM Chk2i (blue), 5 μM ATMi (red), or DMSO (black) added at day 0, day 4, or day 12 after EBV infection. Results shown are the average of four independent normal donors ± SEM.

(G) Efficiency of EBV outgrowth from (F) was calculated, and the average ratio of inhibitor-treated to DMSO-treated infections ± SEM for four normal donors is plotted.

signaling pathway that limited initial B cell proliferation and, consequently, long-term outgrowth into LCLs.

EBV Latent Gene Expression Changes and Consequences in Early Infected Cell Divisions
The dynamic changes in proliferation and DDR-associated gene expression support our cell-based assays indicating an early period of ATM/Chk2-mediated growth suppression that is

attenuated in later divisions enabling long-term LCL outgrowth. However, to determine whether these changes correlated with viral gene expression, we queried viral transcripts and proteins associated with the latency III growth program in sorted PDs after infection (Figure 6 and Figure S5). Wp-associated transcripts were expressed at a markedly higher level than Cp transcripts prior to the first infected cell division (PD0) (Figure 6A). However, this ratio shifted such that Cp levels were greater after three to four cell
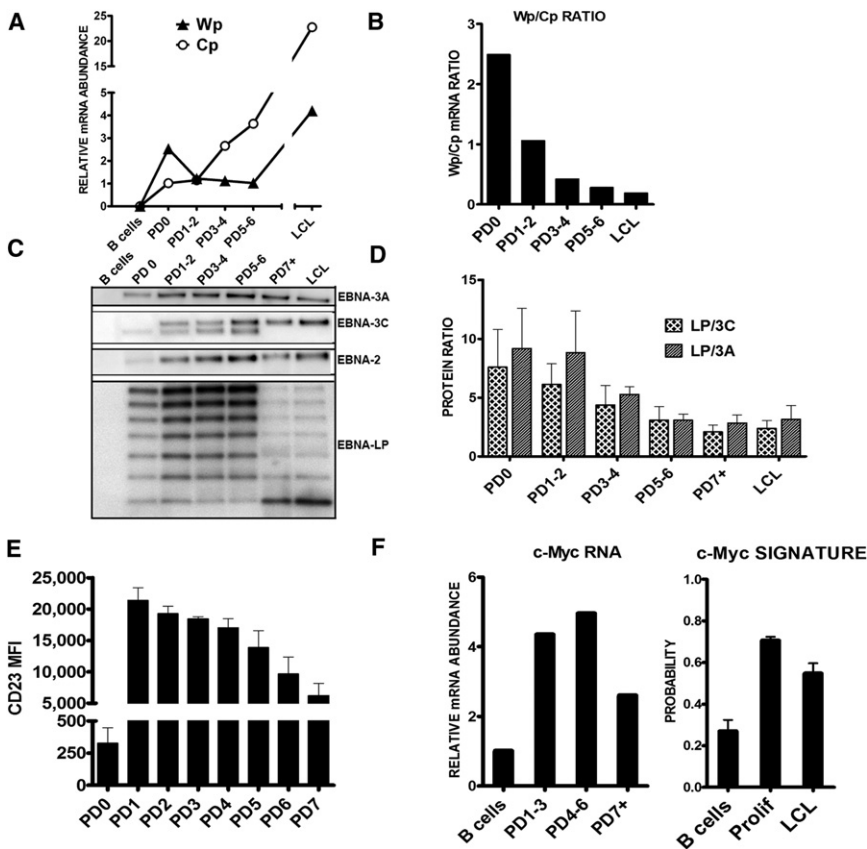
Figure 6. EBV Latency and Consequential Host Gene Expression Changes from Initial B Cell Proliferation through LCL Outgrowth

(A) Expression of Wp (filled triangles)- and Cp (open circles)-derived mRNAs in EBV-infected cells sorted by PD and monoclonal LCLs. Relative mRNA abundance normalized to a β-actin control is plotted versus PD. These data are representative of two normal donors and consistent with published time course experiments (Woisetschlaeger et al., 1989, 1990).

(B) The ratio of Wp to Cp mRNA expression levels from (A) is plotted versus division and through LCL outgrowth.

(C) Protein expression of EBNA-LP, EBNA2, EBNA3A, and EBNA3C are shown from sorted infected PDs and a polyclonal LCL from the same donor.

(D) Proteins detected by western blotting from three independent normal donors similar to those in (C) were quantified. The average ratio of total EBNA-LP protein (i.e., all isoforms) relative to total EBNA3A or EBNA3C ± SEM is plotted versus PD through LCL.

(E) Average CD23 surface expression as mean fluorescence intensity (MFI) is plotted versus PD ± SEM for two donors.

(F) (Left) The expression level of c-Myc mRNA is plotted versus sorted PD. (Right) The activity of the c-Myc target gene expression signature (Bild et al., 2006) is plotted from the average expression of targets in microarray samples from four independent donors of resting B cells (B), early proliferating B cells (Prolif), and monoclonal LCLs. Error bars represent SEM.

divisions and through LCL outgrowth consistent with previous observations (Figure 6B and Schlager et al., 1996; Woisetschlaeger et al., 1989; Woisetschlaeger et al., 1990). The consequence of the high Wp/Cp ratio was heightened levels of EBNA-LP protein as well as a heightened EBNA-LP to EBNA3A and -3C protein ratio in early divisions that waned through LCL outgrowth (Figures 6C and 6D). Thus, the initial cell divisions characterized by hyperproliferation display a distinct EBNA gene expression equilibrium that may affect EBNA2 target gene expression.

To more rigorously assess this, we analyzed EBNA2 targets including CD23 (Wang et al., 1991) and c-Myc (Kaiser et al., 1999). In both cases, these EBNA2 targets were highly induced in early cell divisions and then attenuated through LCL outgrowth, still remaining significantly higher than resting B cell levels (Figures 6E and 6F). The consequences of the transient increase in c-Myc mRNA was manifested in an increase of the c-Myc target gene expression signature (Bild et al., 2006) during early proliferation that was attenuated in LCLs, though still greater than resting B cell levels (Figure 6F). Given the importance in titrating this potentially genotoxic oncoprotein and the known role of ATM in suppressing c-Myc oncogenesis (Hong et al., 2006; Murphy et al., 2008; Pusapati et al., 2006), these findings strongly support a model of acute oncogenic stress early after EBV infection that is modulated through the well-described Wp to Cp switch enabling modest EBNA2 activity critical for indefinite EBV-infected cell outgrowth.

EBNA3C Is Required to Attenuate the EBV-Induced DNA Damage Response

While the induction of the DDR after EBV infection requires latent gene expression and proliferation, a definitive role for viral latent genes in attenuating this response was not demonstrated. In order to determine which latent genes are critical for DDR attenuation during late divisions after infection, we chose to interrogate the EBNA3 proteins, EBNA3A and EBNA3C, as they are known to modulate EBNA2 activity. Infection of primary B cells with EBV B95-8, EBNA3A knockout (KO), or EBNA3C KO virus (Anderton et al., 2008) supported early B cell proliferation (Figures S6A–S6C). However, upon sorting these early proliferating cells we observed that EBNA3C KO virus-infected cells displayed increased activation of the DDR, while EBNA3A KO-infected cells were similar to WT B95-8 infection in DDR activation (Figures 7A and 7B). Indeed, greater than 80% of EBNA3C KO-infected cells were γ-H2AX positive relative to ~50% of WT or EBNA3A KO-infected cells (Figure 7C). Similarly, EBNA3C KO-infected cells accumulated 53BP1 DDR foci to a greater extent than WT or EBNA3A KO-infected cells (p < 0.001, 3C KO versus WT; p > 0.1, 3A KO versus WT). Thus, while B cells infected with either EBNA3A KO or EBNA3C KO virus were crippled for long-term outgrowth (Figures S6B and S6C), these experiments define a critical role for EBNA3C in attenuating the host DDR to EBV infection early after infection. These data strongly support our model of a latent gene expression-triggered hyperproliferation-induced DDR, followed by proper expression
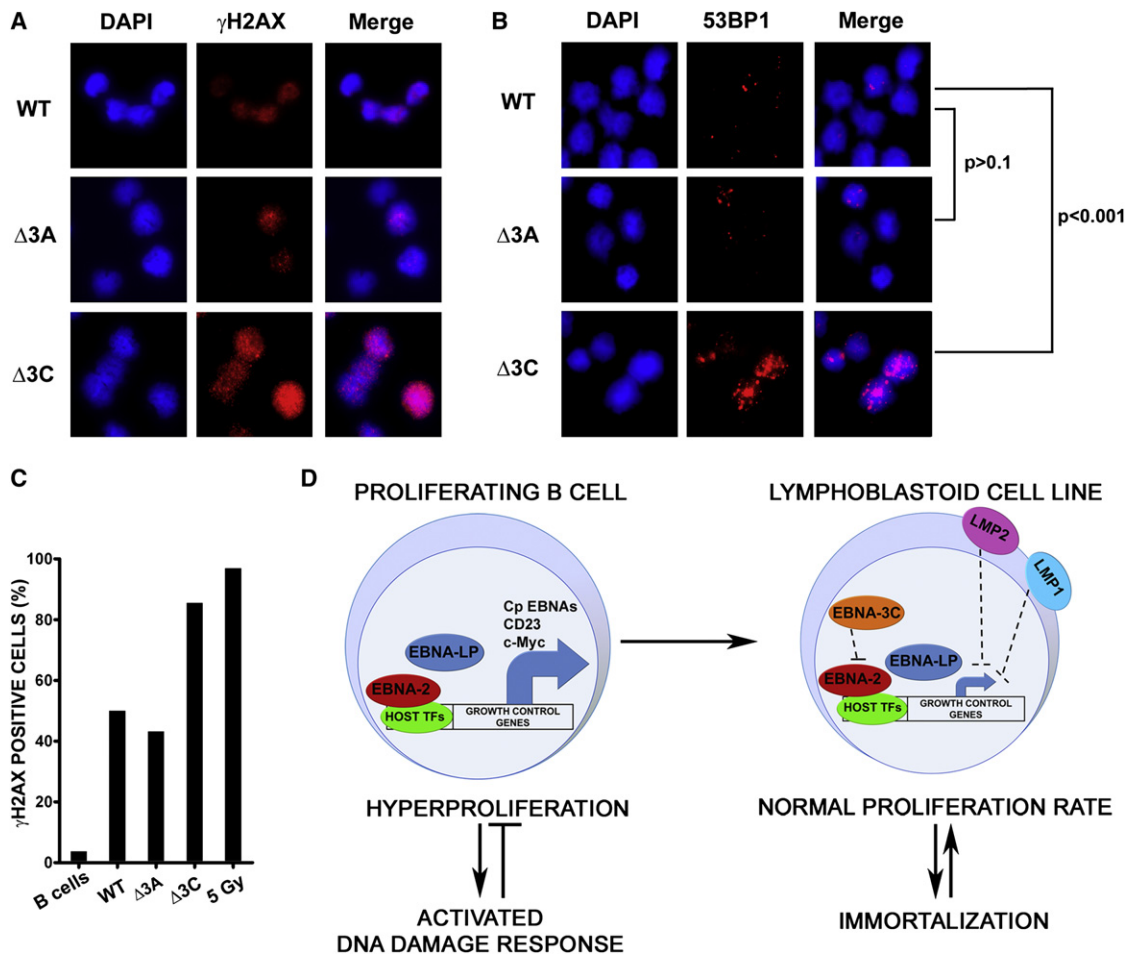
Figure 7. EBNA3C Attenuates the EBV-Induced DNA Damage Response

(A) Representative IF images are shown of γ-H2AX staining (red) from WT, EBNA3A KO (Δ3A), and EBNA3C KO (Δ3C) infected and sorted PD1-4 B cells. DAPI DNA stained (blue) and DAPI/γ-H2AX merged images are also shown.

(B) Representative IF images are shown of 53BP1 staining (red) from WT, Δ3A, and Δ3C infected and sorted PD1-4 B cells.

(C) Quantification of IF data from (A) is plotted as percentage γ-H2AX-positive cells. Average values are plotted for infected cells, uninfected B cells, and 5 Gy γ-irradiated B cells.

(D) Model for EBV-induced DDR/hyperproliferative period and attenuation during LCL outgrowth. Early in infection EBNA2 and EBNA-LP associate with cellular transcription factors (TF) to potently upregulate expression of growth control genes and B cell activation markers, including c-Myc and CD23, activating the host DDR (left). Later in infection, the activity of the EBNA3 proteins, in particular EBNA3C, downregulate EBNA2 function, as LMP1 and LMP2 are upregulated and may cooperate in the constitutive but attenuated expression of host growth control genes and enhanced cell survival (right).

of the EBNA3 proteins, in particular EBNA-3C, in order to attenuate a potentially genotoxic and growth-suppressive signaling pathway (Figure 7D).

DISCUSSION

It has long been recognized that EBV transformation efficiency is on the order of 1%–10% of infected primary human B cells (Henderson et al., 1977; Sugden and Mark, 1977). However, little is known about the molecular mechanism responsible for this low efficiency. We hypothesize that a robust innate tumor suppressor response is activated by latent viral oncoproteins and blocks outgrowth of the majority of infected cells. Recent evidence suggests that activated oncogene expression is sufficient to trigger a growth-suppressive DNA damage responsive

signaling pathway (Halazonetis et al., 2008), and other oncogenic viruses, including the Kaposi's sarcoma-associated herpesvirus, have been shown to induce the DDR after infection or when viral oncoproteins are expressed in primary cells (Dahl et al., 2005; Koopal et al., 2007). Therefore, in this study we asked whether EBV was capable of inducing a DDR in primary B cells and, importantly, whether this response resulted in the low transformation efficiency. We observed that as EBV-infected cells initiated proliferation, a transient DDR was activated as evidenced by phosphorylation of ATM Ser1981, H2AX Ser139 (γ-H2AX), Chk2 Thr68, and accumulation of 53BP1 in nuclear foci. Modulation of this signaling pathway by chemical antagonism of ATM and its downstream target Chk2 markedly increased EBV-mediated B cell polyclonal expansion and transformation efficiency, thereby demonstrating that the DDR

contributes to an EBV-induced innate tumor suppressor pathway. This study identifies a molecular pathway that restricts EBV transformation.

The Source of DNA Damage

Toward characterizing the EBV-induced DNA damage signal, we reasoned that either viral or cellular DNA was important for ATM activation. In addition to oncogenic stress, replication intermediates of DNA viruses and retroviruses contain double-stranded DNA ends that activate ATM (Lilley et al., 2007). In fact, EBV lytic replication induces a DDR which is suppressed by inhibition of downstream transcriptional activation of p53 (Kudoh et al., 2005; Mauser et al., 2002). In our studies of primary B cell infection, however, we found no evidence of viral lytic DNA replication or viral DNA associated with DDR activation. First, we did not observe DDR activation within the first 3 days after EBV infection, nor did we observe activation using UV-inactivated virus or the nontransforming EBV variant P3HR1, suggesting that the incoming linear DNA genome and tegument proteins within the virion were not responsible for this signal. Second, lytic viral DNA was not responsible for DDR activation, as less than 1% of infected cells were undergoing lytic DNA replication when greater than 50% of infected cells were γ-H2AX positive. Third, we asked whether the DNA damage signal was derived from viral episomes since DNA repair factors are recruited to the episome to ensure proper resolution of Holliday junctions following episome replication (Deng et al., 2002; Dheekollu et al., 2007). We observed little increase in episome number per cell and found that viral episomes and γ-H2AX did not colocalize during the period of DDR activation. These data collectively demonstrate that viral DNA is not the source of DNA damage. Our experiments cannot rule out the possibility, however, that viral lytic gene expression downstream of BZLF1 in the absence of lytic DNA replication (Kalla et al., 2010) plays a role in the transient DDR early after infection. Despite this possibility, we inferred from our data that viral latent gene expression causes an oncogenic stress response leading to cellular DNA damage.

The initiation of cell proliferation defines the period after EBV infection when ATM and Chk2 were active in suppressing transformation. Rigorous analysis of infected cell division rates uncovered a period of hyperproliferation where early population doublings (PDs) were every 8–12 hr leading to DDR activation, while later divisions displayed an attenuated rate of ~24–30 hr per division, similar to LCLs, and had little evidence of DDR activation. Microarray analysis of gene expression during the transition from resting B cell to early EBV-induced hyperproliferation and through LCL outgrowth strongly supported our cell-based observations. Specifically, genes involved in proliferation and the DDR, including ATM/p53-dependent targets (Elkon et al., 2005), were highly induced early after infection and then attenuated during the transition to LCL. We propose that aberrant induction of cellular DNA replication early after EBV infection activates a DDR that is dependent on EBNA2- and EBNA-LP-mediated upregulation of S phase promoting oncoproteins including c-Myc, cyclin D2, and E2F1 (Kaiser et al., 1999; Sinclair et al., 1994; and Figure 6). Indeed, we observed increased expression of c-Myc and its gene activation signature in hyperproliferating cells relative to LCLs. Furthermore, EBNA-LP protein levels and Wp-derived transcripts were heightened

during this early period relative to EBNA3 proteins and Cp transcripts, consistent with previous analysis of the initial cascade of viral latent gene expression at different days postinfection (Schlager et al., 1996; Woisetschlaeger et al., 1989, 1990). Finally, EBNA3C- but not EBNA3A-deleted virus-infected cells displayed a significantly stronger DDR during early proliferation. Thus, while both EBNA3A and EBNA3C likely mitigate growth arrest in LCLs through p16 suppression (Hertle et al., 2009; Skalska et al., 2010), during early outgrowth EBNA3C is also required to modulate the DDR. Collectively, our data support a model in which initial EBV-driven hyperproliferation leads to an oncogenic stress that is ultimately attenuated as EBNA3 proteins moderate EBNA2 driven c-Myc expression and its genotoxic and growth suppressive consequences. This ultimate balance in viral and host gene expression enables constitutive S phase induction without driving selection of cells with genomic instability.

In Vivo Implications

Our findings have implications pertaining to the germinal center model for EBV infection (Roughan and Thorley-Lawson, 2009) in the context of B cell lymphomagenesis. In particular, our observed hyperproliferative phase early after infection in vitro may be similarly induced by EBV in vivo and is reminiscent of B cell proliferation rates in the germinal center (MacLennan, 1994). Bcl-6 downregulation of the DDR mitigates the consequences of centroblast hyperproliferation in the germinal center (Ranuncolo et al., 2007), while EBV potently suppresses Bcl-6 early after infection, leaving DDR checkpoints intact (Siemer et al., 2008). In vivo, an EBV-induced hyperproliferative period after primary infection may promote extrafollicular B cell maturation or drive EBV-infected naive B cells into GCs. However, a critical balance must be struck between the aberrant latent oncoprotein-driven proliferation early after infection and the stable proliferative signals found in LCLs to maintain an activated, immortalized state. Perturbations in this balance in vivo may select for mutations driving lymphomagenesis. For example, the *IgH/c-myc* translocation common in BL may be the consequence of such an event. Given our findings, it is plausible that imbalances in EBV latent gene expression may provide a milieu of cells with an increased potential for genomic instability. Recent work in BL cell lines suggests that this is likely the case.

EBV infection of BL cell lines or heterologous expression of EBNA1, EBNA3C, or LMP1 in BL cell lines increased the frequency of nonclonal chromosomal aberrations (Gruhne et al., 2009a, 2009b). EBNA1 increased reactive oxygen species (ROS) through transcriptional upregulation of NOX2, EBNA3C perturbed mitotic spindle checkpoints through BubR1 downregulation, and LMP1 attenuated ATM protein levels and decreased DNA repair. EBNA3C has also been shown to modulate the activity of Chk2 (Choudhuri et al., 2007). However, these three viral proteins are constitutively expressed in LCLs in the absence of overt genomic aberrations. Therefore, we expect that these findings unmask activities that may link the aforementioned potential for imbalanced gene expression to tumorigenesis. In our system, we did not observe increased transformation in the presence of antioxidants including N-acetyl cysteine or citric acid (data not shown), suggesting that EBNA1-induced ROS was not responsible for the EBV-induced DDR. We also

did not observe changes in BubR1 or ATM expression through LCL outgrowth (data not shown). However, we anticipate that genomic instability may ensue in the setting of aberrant latent oncoprotein expression that may exist in BL and other EBV-associated tumors. Consistent with this notion and our findings, a recent report suggests that while LCLs maintain a stable karyotype, early DNA damaging events may lead to nonclonal chromosomal aberrations including telomere fusions (Lacoste et al., 2009). This report supports our findings of an early hyperproliferation-associated oncogenic stress that may induce such structures leading to ATM activation (Karlseder et al., 1999) and suppression of long-term outgrowth. Thus, only cells with the ability to maintain a stable karyotype emerge as LCLs.

Summary

Our study provides the characterization of an innate tumor suppressor pathway that regulates EBV immortalization of B cells. This pathway depends on ATM and Chk2, which are activated early after infection during a period of hyperproliferation. The initial high level expression of EBNA2 and EBNA-LP target genes such as c-Myc leads to DDR activation. Following this initial period, the activity of additional viral latent proteins, including EBNA3C and possibly LMP1 and LMP2, is important for attenuating early gene expression targets, limiting activation of the DDR, and ensuring cell survival. The end result of these dynamic changes in viral and cellular gene expression is outgrowth of a constitutively activated LCL harboring a stable karyotype. However, perturbations in this gene expression program through loss of upstream control by viral latent proteins may lead to the progression of EBV-associated lymphomas. Our studies provide a model for the study of EBV transformation accounting for dynamic viral and host changes during the early period following primary B cell infection.

EXPERIMENTAL PROCEDURES

Antibodies

Primary antibodies to γH2AX, pATM Ser1981, and 53BP1 (Cell Signaling #2577, #4526, and #4937) were used for IF at 1:50. Alexa488 goat α-mouse and Alexa 568 goat α-rabbit were used as secondary antibodies (Molecular Probes #A-11029 and #A-11011). Rabbit α-human Chk2 or pChk2 Thr68 (Cell Signaling #2662 or #2661) and mouse α- EBNA-LP (JF-186, 1:250), EBNA2 (PE2, 1:100), EBNA3A (Exalpha #F115P, 1:500), and EBNA3C (A10, gift of E. Johannsen 1:2500) were used for western blotting.

Fluorescence Microscopy
Immunofluorescence

3×10^5 B cells were pelleted, washed in PBS, resuspended in 25 μl of PBS, spread on a microscope slide and dried at 37°C for 20 min then fixed in 4% PFA in PBS for 15 min, permeabilized in PBS containing 0.5% Tween-20 for 20 min then blocked in PBS with 0.2% Tween-20 containing 5% normal goat serum for 1 hr. Indirect IF was performed as described in Bridger and Lichter (1999). Slides were mounted in Vectashield containing DAPI (Vector Laboratories).

Fluorescence In Situ Hybridization

Cells were fixed in methanol acetic acid as described previously (Sullivan and Warburton, 1999). The EBV genome containing bacterial artificial chromosome MD-1 (kindly provided by F. Wang, Harvard Medical School) was labeled with fluorescent green-dUTP using a nick translation kit (Abbott Molecular) following the manufacturer's instructions. Slides were denatured in 70% formamide, hybridized, and washed as described previously (Sullivan and

Warburton, 1999) except with using fluorescent probes, slides were not blocked then incubated with a fluorescent secondary antibody.

IF/FISH

Slides were fixed for IF in 2% paraformaldehyde in PBS. Antibodies were added to slides and denatured as previously described (Sullivan and Warburton, 1999) except that slides were denatured for 6 min. Slides were hybridized and washed as described above.

Data analysis was performed as described in the Supplemental Experimental Procedures.

Flow Cytometry Analysis
B Cell Proliferation Assays

6-carboxyfluorescein succinimidyl ester (CFSE, Sigma, #21888)-stained or CellTrace Violet (Invitrogen, #C34557)-stained PBMCs were infected with EBV and incubated with different concentrations of ATMi, Chk2i, or DMSO during different periods. Proliferation of CD19+ cells was assayed by flow cytometry as a ratio of CFSE^{low} cells to total PBMCs at 14 days after infection. Detailed kinetics of EBV proliferation was determined as described in Figure S3 (Hawkins et al., 2007).

ACCESSION NUMBERS

SUPPLEMENTAL INFORMATION

ACKNOWLEDGMENTS

REFERENCES

Alfieri, C., Birkenbach, M., and Kieff, E. (1991). Early events in Epstein-Barr virus infection of human B lymphocytes. Virology *181*, 595–608.

Anderton, E., Yee, J., Smith, P., Crook, T., White, R.E., and Allday, M.J. (2008). Two Epstein-Barr virus (EBV) oncoproteins cooperate to repress expression of the proapoptotic tumour-suppressor Bim: clues to the pathogenesis of Burkitt's lymphoma. Oncogene *27*, 421–433.

Arienti, K.L., Brunmark, A., Axe, F.U., McClure, K., Lee, A., Blevitt, J., Neff, D.K., Huang, L., Crawford, S., Pandit, C.R., et al. (2005). Checkpoint kinase inhibitors: SAR and radioprotective properties of a series of 2-arylbenzimidazoles. J. Med. Chem. *48*, 1873–1885.

Bartkova, J., Horejsi, Z., Koed, K., Kramer, A., Tort, F., Zieger, K., Guldberg, P., Sehested, M., Nesland, J.M., Lukas, C., et al. (2005). DNA damage response as a candidate anti-cancer barrier in early human tumorigenesis. Nature *434*, 864–870.

Bartkova, J., Rezaei, N., Liontos, M., Karakaidos, P., Kletsas, D., Issaeva, N., Vassiliou, L.V., Kolettas, E., Niforou, K., Zoumpourlis, V.C., et al. (2006). Oncogene-induced senescence is part of the tumorigenesis barrier imposed by DNA damage checkpoints. Nature *444*, 633–637.

Bild, A.H., Yao, G., Chang, J.T., Wang, Q., Potti, A., Chasse, D., Joshi, M.B., Harpole, D., Lancaster, J.M., Berchuck, A., et al. (2006). Oncogenic pathway signatures in human cancers as a guide to targeted therapies. Nature *439*, 353–357.

Bridger, J.M., and Lichter, P. (1999). Analysis of mammalian interphase chromosomes by FISH and immunofluorescence. In Chromosome Structural Analysis, W.A. Bickmore, ed. (Oxford: Oxford University Press), pp. 103–121.

Chang, J.T., and Nevins, J.R. (2006). GATHER: a systems approach to interpreting genomic signatures. Bioinformatics *22*, 2926–2933.

Choudhuri, T., Verma, S.C., Lan, K., Murakami, M., and Robertson, E.S. (2007). The ATM/ATR signaling effector Chk2 is targeted by Epstein-Barr virus nuclear antigen 3C to release the G2/M cell cycle block. J. Virol. *81*, 6718–6730.

Dahl, J., You, J., and Benjamin, T.L. (2005). Induction and utilization of an ATM signaling pathway by polyomavirus. J. Virol. *79*, 13007–13017.

Deng, Z., Lezina, L., Chen, C.J., Shtivelband, S., So, W., and Lieberman, P.M. (2002). Telomeric proteins regulate episomal maintenance of Epstein-Barr virus origin of plasmid replication. Mol. Cell *9*, 493–503.

Dheekollu, J., Deng, Z., Wiedmer, A., Weitzman, M.D., and Lieberman, P.M. (2007). A role for MRE11, NBS1, and recombination junctions in replication and stable maintenance of EBV episomes. PLoS ONE *2*, e1257. 10.1371/journal.pone.0001257.

Di Micco, R., Fumagalli, M., Cicalese, A., Piccinin, S., Gasparini, P., Luise, C., Schurra, C., Garre, M., Nuciforo, P.G., Bensimon, A., et al. (2006). Oncogene-induced senescence is a DNA damage response triggered by DNA hyper-replication. Nature *444*, 638–642.

Elkon, R., Rashi-Elkeles, S., Lerenthal, Y., Linhart, C., Tenne, T., Amariglio, N., Rechavi, G., Shamir, R., and Shiloh, Y. (2005). Dissection of a DNA-damage-induced transcriptional network using a combination of microarrays, RNA interference and computational promoter analysis. Genome Biol. *6*, R43.

Gorgoulis, V.G., Vassiliou, L.V., Karakaidos, P., Zacharatos, P., Kotsinas, A., Liloglou, T., Venere, M., Ditullio, R.A., Jr., Kastrinakis, N.G., Levy, B., et al. (2005). Activation of the DNA damage checkpoint and genomic instability in human precancerous lesions. Nature *434*, 907–913.

Gruhne, B., Sompallae, R., Marescotti, D., Kamranvar, S.A., Gastaldello, S., and Masucci, M.G. (2009a). The Epstein-Barr virus nuclear antigen-1 promotes genomic instability via induction of reactive oxygen species. Proc. Natl. Acad. Sci. USA *106*, 2313–2318.

Gruhne, B., Sompallae, R., and Masucci, M.G. (2009b). Three Epstein-Barr virus latency proteins independently promote genomic instability by inducing DNA damage, inhibiting DNA repair and inactivating cell cycle checkpoints. Oncogene *28*, 3997–4008.

Halazonetis, T.D., Gorgoulis, V.G., and Bartek, J. (2008). An oncogene-induced DNA damage model for cancer development. Science *319*, 1352–1355.

Hawkins, E.D., Hommel, M., Turner, M.L., Battye, F.L., Markham, J.F., and Hodgkin, P.D. (2007). Measuring lymphocyte proliferation, survival and differentiation using CFSE time-series data. Nat. Protoc. *2*, 2057–2067.

Henderson, E., Miller, G., Robinson, J., and Heston, L. (1977). Efficiency of transformation of lymphocytes by Epstein-Barr virus. Virology *76*, 152–163.

Hertle, M.L., Popp, C., Petermann, S., Maier, S., Kremmer, E., Lang, R., Mages, J., and Kempkes, B. (2009). Differential gene expression patterns of EBV infected EBNA-3A positive and negative human B lymphocytes. PLoS Pathog. *5*, e1000506. 10.1371/journal.ppat.1000506.

Hickson, I., Zhao, Y., Richardson, C.J., Green, S.J., Martin, N.M., Orr, A.I., Reaper, P.M., Jackson, S.P., Curtin, N.J., and Smith, G.C. (2004). Identification and characterization of a novel and specific inhibitor of the ataxia-telangiectasia mutated kinase ATM. Cancer Res. *64*, 9152–9159.

Hong, S., Pusapati, R.V., Powers, J.T., and Johnson, D.G. (2006). Oncogenes and the DNA damage response: Myc and E2F1 engage the ATM signaling pathway to activate p53 and induce apoptosis. Cell Cycle *5*, 801–803.

Kaiser, C., Laux, G., Eick, D., Jochner, N., Bornkamm, G.W., and Kempkes, B. (1999). The proto-oncogene c-myc is a direct target gene of Epstein-Barr virus nuclear antigen 2. J. Virol. *73*, 4481–4484.

Kalla, M., Schmeinck, A., Bergbauer, M., Pich, D., and Hammerschmidt, W. (2010). AP-1 homolog BZLF1 of Epstein-Barr virus has two essential functions

dependent on the epigenetic state of the viral genome. Proc. Natl. Acad. Sci. USA *107*, 850–855.

Karlseder, J., Broccoli, D., Dai, Y., Hardy, S., and de Lange, T. (1999). p53- and ATM-dependent apoptosis induced by telomeres lacking TRF2. Science *283*, 1321–1325.

Kieff, E., and Rickinson, A. (2006). Epstein-Barr virus and its replication. In Fields Virology, D.M. Knipe and P.M. Howley, eds. (Philadelphia: Lippincott, Williams, and Wilkins), pp. 2603–2654.

Koopal, S., Furuhjelm, J.H., Jarviluoma, A., Jaamaa, S., Pyakurel, P., Pussinen, C., Wirzenius, M., Biberfeld, P., Alitalo, K., Laiho, M., et al. (2007). Viral oncogene-induced DNA damage response is activated in Kaposi sarcoma tumorigenesis. PLoS Pathog. *3*, 1348–1360.

Kudoh, A., Fujita, M., Zhang, L., Shirata, N., Daikoku, T., Sugaya, Y., Isomura, H., Nishiyama, Y., and Tsurumi, T. (2005). Epstein-Barr virus lytic replication elicits ATM checkpoint signal transduction while providing an S-phase-like cellular environment. J. Biol. Chem. *280*, 8156–8163.

Lacoste, S., Wiechec, E., Dos Santos Silva, A.G., Guffei, A., Williams, G., Lowbeer, M., Benedek, K., Henriksson, M., Klein, G., and Mai, S. (2009). Chromosomal rearrangements after ex vivo Epstein-Barr virus (EBV) infection of human B cells. Oncogene *29*, 503–515.

Lilley, C.E., Schwartz, R.A., and Weitzman, M.D. (2007). Using or abusing: viruses and the cellular DNA damage response. Trends Microbiol. *15*, 119–126.

MacLennan, I.C. (1994). Germinal centers. Annu. Rev. Immunol. *12*, 117–139.

Mauser, A., Saito, S., Appella, E., Anderson, C.W., Seaman, W.T., and Kenney, S. (2002). The Epstein-Barr virus immediate-early protein BZLF1 regulates p53 function through multiple mechanisms. J. Virol. *76*, 12503–12512.

Murphy, D.J., Junttila, M.R., Pouyet, L., Karnezis, A., Shchors, K., Bui, D.A., Brown-Swigart, L., Johnson, L., and Evan, G.I. (2008). Distinct thresholds govern Myc's biological output in vivo. Cancer Cell *14*, 447–457.

Pusapati, R.V., Rounbehler, R.J., Hong, S., Powers, J.T., Yan, M., Kiguchi, K., McArthur, M.J., Wong, P.K., and Johnson, D.G. (2006). ATM promotes apoptosis and suppresses tumorigenesis in response to Myc. Proc. Natl. Acad. Sci. USA *103*, 1446–1451.

Ranuncolo, S.M., Polo, J.M., Dierov, J., Singer, M., Kuo, T., Greally, J., Green, R., Carroll, M., and Melnick, A. (2007). Bcl-6 mediates the germinal center B cell phenotype and lymphomagenesis through transcriptional repression of the DNA-damage sensor ATR. Nat. Immunol. *8*, 705–714.

Roughan, J.E., and Thorley-Lawson, D.A. (2009). The intersection of Epstein-Barr virus with the germinal center. J. Virol. *83*, 3968–3976.

Schlager, S., Speck, S.H., and Woisetschlager, M. (1996). Transcription of the Epstein-Barr virus nuclear antigen 1 (EBNA1) gene occurs before induction of the BCR2 (Cp) EBNA gene promoter during the initial stages of infection in B cells. J. Virol. *70*, 3561–3570.

Siemer, D., Kurth, J., Lang, S., Lehnerdt, G., Stanelle, J., and Kuppers, R. (2008). EBV transformation overrides gene expression patterns of B cell differentiation stages. Mol. Immunol. *45*, 3133–3141.

Sinclair, A.J., Palmero, I., Peters, G., and Farrell, P.J. (1994). EBNA-2 and EBNA-LP cooperate to cause G0 to G1 transition during immortalization of resting human B lymphocytes by Epstein-Barr virus. EMBO J. *13*, 3321–3328.

Skalska, L., White, R.E., Franz, M., Ruhmann, M., and Allday, M.J. (2010). Epigenetic repression of p16(INK4A) by latent Epstein-Barr virus requires the interaction of EBNA3A and EBNA3C with CtBP. PLoS Pathog. *6*, e1000951.

Stiff, T., Walker, S.A., Cerosaletti, K., Goodarzi, A.A., Petermann, E., Concannon, P., O'Driscoll, M., and Jeggo, P.A. (2006). ATR-dependent phosphorylation and activation of ATM in response to UV treatment or replication fork stalling. EMBO J. *25*, 5775–5782.

Stracker, T.H., Couto, S.S., Cordon-Cardo, C., Matos, T., and Petrini, J.H. (2008). Chk2 suppresses the oncogenic potential of DNA replication-associated damage. Mol. Cell *31*, 21–32.

Sugden, B., and Mark, W. (1977). Clonal transformation of adult human leukocytes by Epstein-Barr virus. J. Virol. *23*, 503–508.

Sullivan, B.A., and Warburton, P.E. (1999). Studying progression of vertebrate chroosomes through mitosis by immunofluorescence and FISH. In

Chromosome Structural Analysis, W.A. Bickmore, ed. (Oxford: Oxford University Press), pp. 81–100.

Szekely, L., Pokrovskaja, K., Jiang, W.Q., Selivanova, G., Lowbeer, M., Ringertz, N., Wiman, K.G., and Klein, G. (1995). Resting B-cells, EBV-infected B-blasts and established lymphoblastoid cell lines differ in their Rb, p53 and EBNA-5 expression patterns. Oncogene *10*, 1869–1874.

Wang, F., Tsang, S.F., Kurilla, M.G., Cohen, J.I., and Kieff, E. (1990). Epstein-Barr virus nuclear antigen 2 transactivates latent membrane protein LMP1. J. Virol. *64*, 3407–3416.

Wang, F., Kikutani, H., Tsang, S.F., Kishimoto, T., and Kieff, E. (1991). Epstein-Barr virus nuclear protein 2 transactivates a cis-acting CD23 DNA element. J. Virol. *65*, 4101–4106.

Woisetschlaeger, M., Strominger, J.L., and Speck, S.H. (1989). Mutually exclusive use of viral promoters in Epstein-Barr virus latently infected lymphocytes. Proc. Natl. Acad. Sci. USA *86*, 6498–6502.

Woisetschlaeger, M., Yandava, C.N., Furmanski, L.A., Strominger, J.L., and Speck, S.H. (1990). Promoter switching in Epstein-Barr virus during the initial stages of infection of B lymphocytes. Proc. Natl. Acad. Sci. USA *87*, 1725–1729.

Zimber-Strobl, U., Kremmer, E., Grasser, F., Marschall, G., Laux, G., and Bornkamm, G.W. (1993). The Epstein-Barr virus nuclear antigen 2 interacts with an EBNA2 responsive cis-element of the terminal protein 1 gene promoter. EMBO J. *12*, 167–175.